



# In vivo study on biocompatibility and bonding strength of Ti/Ti–20 vol.% HA/Ti–40 vol.% HA functionally graded biomaterial with bone tissues in the rabbit

Chenglin Chu <sup>a,\*</sup>, Xiaoyan Xue <sup>b</sup>, Jingchuan Zhu <sup>c</sup>, Zhongda Yin <sup>c</sup>

<sup>a</sup> School of Materials Science and Engineering, Southeast University, Nanjing 210096, China

<sup>b</sup> General Medicine Centre, Zhong Da Hospital, Southeast University, Nanjing 210009, China

<sup>c</sup> School of Materials Science and Engineering, Harbin Institute of Technology, Box 433, Harbin 150001, China

Received 29 June 2005; received in revised form 21 March 2006; accepted 27 March 2006

## Abstract

Ti/Ti–20 vol.% HA/Ti–40 vol.% HA functionally graded biomaterial (FGM) was fabricated by a hot-pressing technique. Then the comprehensive biocompatibility and bonding strength of the FGM with bone tissues in the rabbit were systematically investigated by in vivo studies in comparison with those of Ti metal. The microstructure of sintered FGM varied gradually from Ti side to Ti–40 vol.% HA side with a graded distribution of each element. There are some fibrous tissues existing at the interface between Ti implant and newborn bones at 4 weeks in vivo. Contrarily new bone tissues can contact directly with Ti–40 vol.% HA graded layer in the FGM at or after 4 weeks in vivo. At 8 weeks, the bonding interfaces between Ti–40 vol.% HA graded layer in the FGM and new bones cannot already be distinguished and the FGM was osseointegrated fully with bone tissues into one bony body. During all implanting periods, the increasing rate of bonding strength for the FGM is higher than that of pure Ti. At 3 months in vivo, the shear fracture for Ti–40 vol.% HA graded layer in the FGM implants occurred in new bone tissues zones near the interface between the FGM implants and bones tissues. The bonding strength of the FGM implants could even exceed the shear strength of new bone tissues (4.73 MPa). Obviously the FGM has better biocompatibility and osseointegration abilities than Ti metal, especially during the early stage after the implantation, which can be due to the existence of the graded layers mixed by HA and Ti. Therefore, it is a promising biomaterial for hard tissue replacement.

© 2006 Elsevier B.V. All rights reserved.

**Keywords:** Hydroxyapatite; Titanium; Functionally graded biomaterial; Biocompatibility; Osseointegration

## 1. Introduction

Although hydroxyapatite (HA,  $\text{Ca}_{10}(\text{PO}_4)_6(\text{OH})_2$ ) has excellent biocompatibility, it is not suitable for hard tissue replacement due to its poor mechanical properties and low reliability [1–6]. At the same time, titanium (Ti) and its alloys with high strength are the preferred metal materials for dentistry and orthopaedics [7,8], however, they are bioinert biomaterials and cannot directly bond to the bone. Moreover, HA coatings to improve the surface bioactivity of titanium metal often flake off as a result of poor macroscopic interface bond between ceramic and metal. The problems above-mentioned can be solved better by fabricating HA–Ti functionally graded biomaterials [9–11].

The concept of functionally graded material (FGM) was initially proposed as a new super heat-resistant material for the next generation of space plane in the 21st century [12,13]. The gradual distribution of components in the FGM can eliminate the macroscopic interface such as that in a direct joint of two materials. FGMs have many potential applications in various fields including dentistry and orthopaedics. For example, HA–Ti FGM can make full use of excellent bioactivity of HA and high strength and toughness of Ti metal [9–11].

So far, both HA–Ti asymmetrical FGM with an asymmetrically distributing compositional profile varying gradually from Ti side to HA side [11] and HA–Ti symmetrical FGM with a symmetrically distributing compositional profile [10] have been developed successfully by our group using a hot-pressing technique. The perfect HA–Ti asymmetrical and symmetrical FGMs were prepared by structure optimization [10,11]. The mechanical properties, fracture behaviors and the relaxing

\* Corresponding author.

E-mail address: clchu@seu.edu.cn (C. Chu).

characteristics of thermal residual stress of HA-Ti FGMs have also been reported correspondingly [9–11].

Although both pure HA ceramic and pure Ti metal have been verified to be the ideal biomaterials with good biocompatibility and have been used extensively in clinical medicine [1–8], the biological properties of the FGMs with Ti metal and HA ceramic as the predominant phases must be determined. Systematic studies on the comprehensive biological properties of HA-Ti FGMs have not been reported.

In this paper, Ti/Ti–20 vol.% HA/Ti–40 vol.% HA FGM with a distributed compositional profile varying from Ti side to Ti–40 vol.% HA side suitable for artificial tooth roots was fabricated by a hot-pressing technique [10,11]. The comprehensive biocompatibility and bonding strength of the FGM with bone tissues in the rabbit were systematically investigated by *in vivo* studies and discussed.

## 2. Experimental procedure

### 2.1. Raw materials and fabrication of Ti/Ti–20 vol.% HA/Ti–40 vol.% HA FGM

The raw materials used for the fabrication of the FGM were HA powders and titanium powders. HA powders were prepared by the reaction between  $\text{Ca}(\text{NO}_3)_2$  and  $(\text{NH}_4)_2\text{HPO}_4$ . Its Ca/P ratio was  $1.67 \pm 2.0\%$  and the content of heavy metals, such as Pb, As, Hg and Cd is less than 1.0 ppm. Sizing by means of Laser Particle Sizer (OMEC LS-POP(III)) showed HA particles have an average size of  $1.75 \mu\text{m}$ . There are significant agglomerations of HA powders shown by scanning electron microscopy (SEM). The chemical composition of titanium powders was (wt.%): Ti 99.3, Fe 0.039, O 0.35, N 0.035, C 0.025, Cl 0.034, H 0.024 and Si 0.0018. The average size of Ti particles is  $45.2 \mu\text{m}$ . The starting powders with different HA/Ti mixing ratios were first blended by ball milling for 12 h. Then the mixed powders were stacked layer by layer in a steel die according to the pre-designed compositional profile of Ti/Ti–20 vol.% HA/Ti–40 vol.% HA FGM as shown in Fig. 1 and compacted at 200 MPa. Finally, green compacts were hot-pressed at  $1100^\circ\text{C}$  under a pressure of 20 MPa in nitrogen atmosphere for 30 min with a heating rate of

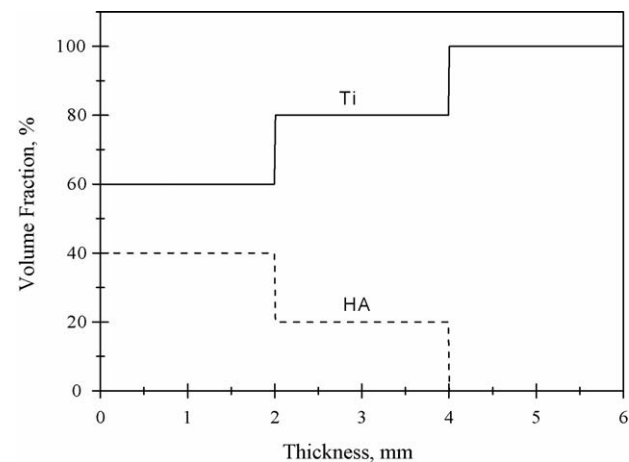


Fig. 1. Pre-designed compositional profile of Ti/Ti–20 vol.% HA/Ti–40 vol.% HA FGM.

$10^\circ\text{C}/\text{min}$  and a cooling rate of  $6^\circ\text{C}/\text{min}$ . Dense pure Ti metal in contrast with the FGM was also produced in the same way.

### 2.2. Characterization

Samples for microstructure observations were cut with a diamond saw, and their surfaces were ground and polished. The microstructure was examined using optical microscope and scanning electron microscope (SEM). The surface distribution of chemical compositions in the FGM was examined using a scanning electron microscope with energy-dispersive analysis by X-rays (EDAX) facility. The phase constitution was analyzed by X-ray diffraction (XRD).

### 2.3. In vivo study

#### 2.3.1. Implant preparation and surgical operation

As shown in Fig. 2a, FGM and pure Ti metal were cut into rectangular specimens about  $3.3 \text{ mm} \times 3.3 \text{ mm} \times 6 \text{ mm}$  in dimension using a diamond saw. The cross-sectional view of the predrilled hole with implant in the skull of New Zealand White rabbits of 2.5 kg weight is illustrated in Fig. 2b. The defec-

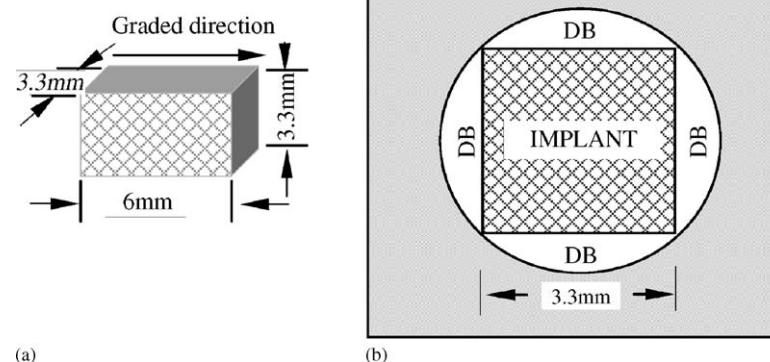


Fig. 2. Schematic configuration of the implant model. (a) Rectangular specimen for implantation; (b) cross-sectional view of the predrilled hole with implant in the skull (DB, defective bone region).

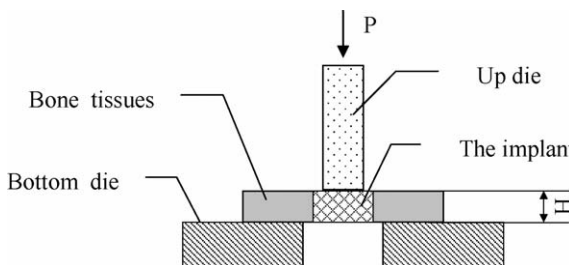


Fig. 3. Schematic diagram for testing shear bonding strength between bone tissues and the implant.

tive bone (DB) region was designed for bone healing. Before implantation, all implants were cleaned with distilled water and sterilized by autoclaving at 121 °C for 30 min. Prophylactic antibiotic was given once during operation. The rectangular implants were inserted into predrilled holes of 4.76 mm diameter using sterile surgical techniques. A total of 80 implants (40 each of FGM and pure Ti metal) were inserted uniformly into the skulls of 10 New Zealand White rabbit of 2.5 kg weight. With implants randomly distributed, each rabbit contained eight implants (four each of FGM and pure Ti metal). At 2, 4, 8, 12 or 28 weeks, two rabbits were sacrificed and the harvested samples were distributed into three parts.

### 2.3.2. Observations of tissues and interfaces between bone and implants

The first parts of the harvested samples were fixed in glutaraldehyde, washed with PBS, then fixed by osmic acid and washed with PBS again, finally dehydrated and evaporated at critical point. The treated samples were covered with a thin film of gold by vacuum-deposition and then observed by SEM.

The second parts of the harvested samples were fixed in 10% buffered formalin. The fixed samples were decalcified in an acid compound (1000 ml solution containing 8.5 g sodium chloride, 100 ml formalin, 70 ml 37% hydrochloric acid, 80 ml formic acid, 40 g aluminum chloride and 25 ml acetic acid glacial). Dehydrated in alcohol and embedded in paraffin, decalcified sections were stained with haematoxylin and eosin (HE) and then examined by light microscopic observation.

### 2.3.3. Measurement of bonding strength of implants with bones

The third parts of the harvested samples were fixed in 10% buffered formalin for shear bonding strength tests. The tested samples were cut by a diamond grinding wheel. Schematic diagram for testing shear bonding strength between bone tissues and the implant is shown in Fig. 3. The loading rate is about 5 mm/min. The shear bonding strength between bone tissues and the implant could be calculated by the following expression:

$$\tau = \frac{P}{4 \times A \times H} \quad (1)$$

where  $A$  is the side length of square cross-section of the implant (about 3.3 mm),  $H$  the average effective thickness of the cortex bone bonding with the implant,  $P$  the maximal extruding force of the implant and  $\tau$  is the shear bonding strength between

bone tissues and the implant. The shear fracture surfaces of the implants at 3 months in vivo were covered with a thin film of gold by vacuum-deposition and then examined by SEM.

## 3. Results and discussion

### 3.1. Fabrication and biocompatibility of Ti/Ti–20 vol.% HA/Ti–40 vol.% HA FGM

Ti/Ti–20 vol.% HA/Ti–40 vol.% HA FGM with the pre-designed compositional profile as shown in Fig. 1 was fabricated by hot pressing. The sintered sample had no bending deformation and microcracks on the surfaces. Fig. 4 shows the optical sectional micrograph of Ti/Ti–20 vol.% HA/Ti–40 vol.% HA FGM, in which the white phase is titanium and the dark one is HA. The microstructure of sintered FGM varied gradually from Ti side to Ti–40 vol.% HA side with the diversification of chemical compositions. The distinct interfaces like those in HA/Ti direct bonding disappears. Even on the sections between the layers of FGM where chemical compositions jumped in a stepwise way, both HA and Ti components are continuous in microstructure.

The phase constitution analyzed by X-ray diffraction indicates that Ti and HA phases are the predominant phases in sintered FGM, and no reactions between HA and Ti are detected. However, a small quantity of decomposed phases of HA, such as  $\alpha$ -Ca<sub>3</sub>(PO<sub>4</sub>)<sub>2</sub> ( $\alpha$ -TCP) and Ca<sub>4</sub>O(PO<sub>4</sub>)<sub>2</sub> could be found in the layers mixed by HA and Ti. To realize the actual distributions of Ca, P and Ti elements, the surface distribution of each element in the FGM was examined using EDAX. Fig. 5 shows the elemental distribution actual profile of the FGM. It could be found that each element in the FGM exhibits a graded distribution. The contents of Ca and P decrease gradually from left to right, while the content of Ti changes contrarily. Their varying tends are basically consistent with those of the designed compositional distribution as shown in Fig. 1.

The interfacial morphology between the implant and newborn bones after different time in vivo was observed using light

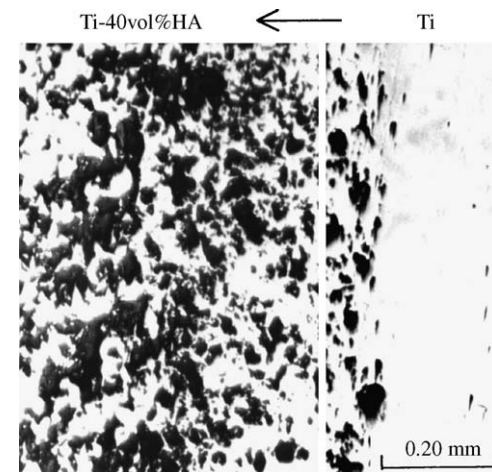


Fig. 4. Optical sectional micrograph of Ti/Ti–20 vol.% HA/Ti–40 vol.% HA functionally graded biomaterial.

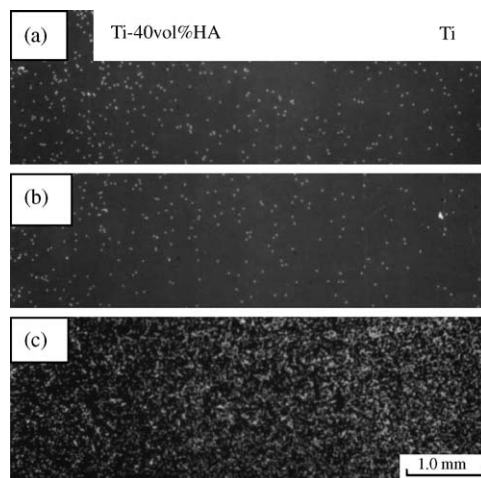


Fig. 5. Distribution of chemical compositions of Ti/Ti-20 vol.% HA/Ti-40 vol.% HA functionally graded biomaterial by SEM surface analysis. (a) Ca; (b) P; (c) Ti.

microscopy after staining with haematoxylin and eosin (HE) as shown in Fig. 6. At 4 weeks in vivo, DB regions around both Ti metal and the FGM implants were filled with newborn osteoid (Fig. 6a and b). However, it could be found that Ti-40 vol.% HA graded layer in the FGM could contact directly with newborn bone tissues (Fig. 6b), while there are some fibrous tissues existing at the interface between Ti metal implants and new-

born bones (Fig. 6a). As shown in Fig. 6c and d, the contacting growth of new bones could be attained for both Ti metal and Ti-40 vol.% HA graded layer in the FGM after 8 weeks in vivo. At 28 weeks in vivo, new bone tissues in DB regions around both Ti metal and Ti-40 vol.% HA graded layer in the FGM implants were maturer than those of 8 weeks (Fig. 6e and f).

After the surgical operation of the implantation in this work, the incisions in the skull of New Zealand White rabbits healed up normally without infection, which suggests indirectly that Ti/Ti-20 vol.% HA/Ti-40 vol.% HA FGM has good biocompatibility and no toxicity to cells. The prophase reaction of body tissues to the implants is the defensive reaction, while the anaphase one is the repairing reaction. From Fig. 6, it could be found that newborn bones between host bones and the FGM implant grew actively and had a growing trend from the brim of host bones to the implants, which indicates that no strong defensive reaction to the FGM implant appears for body tissues and cells. Moreover, the FGM has no bad effects on the repairing reaction of body tissues and can promote the regeneration of bones. After 8 weeks in vivo, the bonding interfaces between Ti-40 vol.% HA graded layer in the FGM and new bones cannot already be distinguished as shown in Fig. 6d. The experimental results indicate farther that the FGM has good affinity and biocompatibility with bone tissues and cells.

It is generally accepted that there are two modes for the implants to affect the generation of bone tissues: one is osteoconduction, the other is osteoinduction [3,7,14–17]. Ti metal and

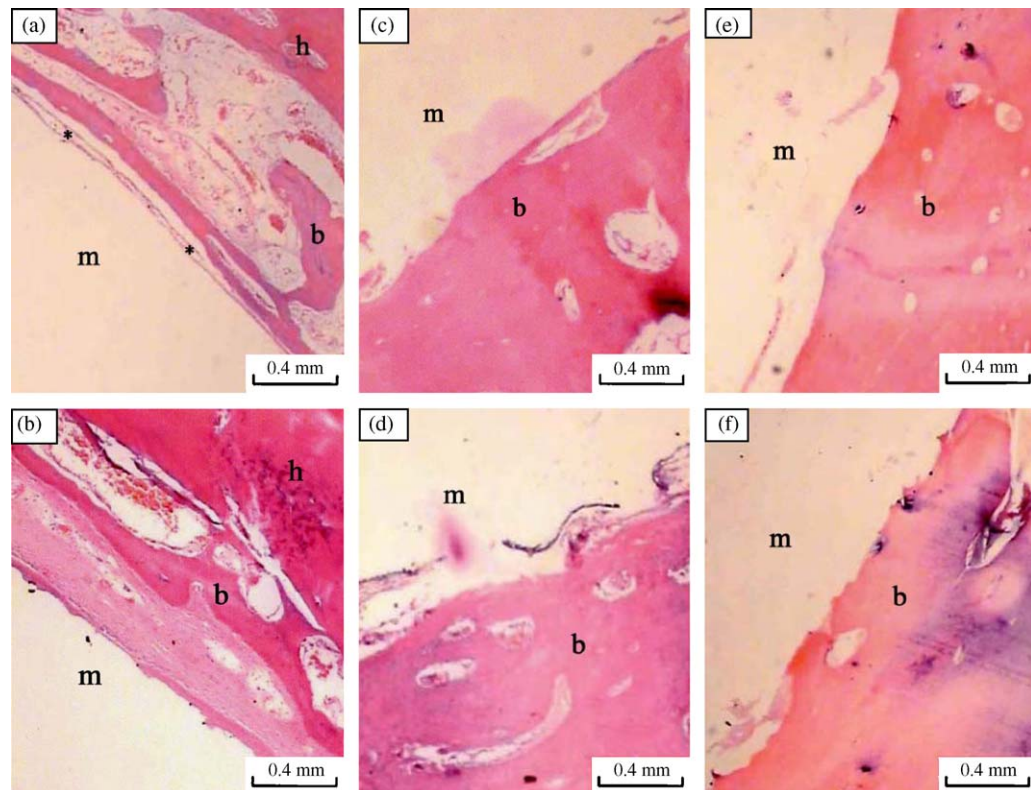


Fig. 6. Interfacial morphology between the implant and newborn bones after different time in vivo observed using light microscopic after stained with haematoxylin and eosin (HE). (a) Pure Ti, 4 weeks; (b) Ti-40 vol.% HA graded layer in the FGM, 4 weeks; (c) pure Ti, 8 weeks; (d) Ti-40 vol.% HA graded layer in the FGM, 8 weeks; (e) pure Ti, 28 weeks; (f) Ti-40 vol.% HA graded layer in the FGM, 28 weeks. m, implant; b, newborn bone; h, host bone; \*, fibrous tissue.

dense HA ceramic can affect the regeneration of bones by the osteoconduction mode [3,7,14–17]. The FGM consists mainly of HA and Ti phases. Only a small quantity of the decomposed products of HA phase, namely the biodegradable  $\alpha$ -TCP and  $\text{Ca}_4\text{O}(\text{PO}_4)_2$ , appeared in the graded layers mixed by HA and Ti in the FGM. No other compounds came into being during the fabrication process. Therefore, the FGM can possess good osteoconduction ability in theory, which can also be verified by *in vivo* studies as shown in Fig. 6.

On the relationship between the implants and bone tissues, the osseointegration concept was proposed [7]. The osseointegration of the implant with bone tissues means that newborn bone tissues can grow into any spaces on the surface of the implants and contact with the implant directly, and no any fibrous tissues present at the interfaces between the implants and bone tissues. It is generally accepted that dense HA ceramic and pure Ti metal can osseointegrate with bone tissues [3,7]. In this work, although both Ti metal and the FGM implants could integrate with bone finally, there are some fibrous tissues existing at the partial interface between pure Ti implant and newborn bone at 4 weeks *in vivo* (Fig. 6a). The contacting growth of new bones with Ti metal appeared after 8 weeks. By contraries, new bone tissues can contact directly with Ti-40 vol.% HA graded layer in the FGM at or after 4 weeks *in vivo* (Fig. 6b, d and f). This indicates that the osseointegration ability of the graded layers mixed by HA and Ti in the FGM is better than that of pure Ti metal during the beginning period of the implantation.

The biodegradable  $\alpha$ -TCP and  $\text{Ca}_4\text{O}(\text{PO}_4)_2$  decomposed from HA phases in the graded layers mixed by HA and Ti have a higher biodegradation rate than HA phase in the biological environment [3,18–20]. The mild dissolution of the decomposition products of HA phase can promote the farther degradation of HA phases by increasing the contacting areas of HA component in the FGM with the body fluid and provide a Ca/P environment with  $\text{Ca}^{2+}$  and  $\text{PO}_4^{3-}$  needed for bone formation [21,22].

### 3.2. Bonding strength of Ti/Ti-20 vol.% HA/Ti-40 vol.% HA FGM with bone tissues

Fig. 7 shows the changes of shear bonding strength between bone tissues and the implants with the implanting time. It could be found that at 2 weeks *in vivo*, the bonding strength of pure Ti implants is the lowest and only 0.44 MPa, while that of the FGM implants can reach 1.75 times that of pure Ti. The experimental results indicate that the osteoconduction and osseointegration abilities of the FGM are better than those of pure Ti metal during the early stage after the implantation. At 3 months, the bonding strength of pure Ti and the FGM implants is 2.03 and 4.73 MPa, respectively. Fig. 8 shows the increasing rates of bonding strength of the implants during different implanting periods. From Figs. 7 and 8, it could be easily found that during all implanting periods, the bonding strength of pure Ti implants increases linearly and slowly and the increasing rate of bonding strength for the FGM is higher than that of pure Ti. After 3 months *in vivo*, the bonding strength of the FGM implants is further higher than that of pure Ti implants.

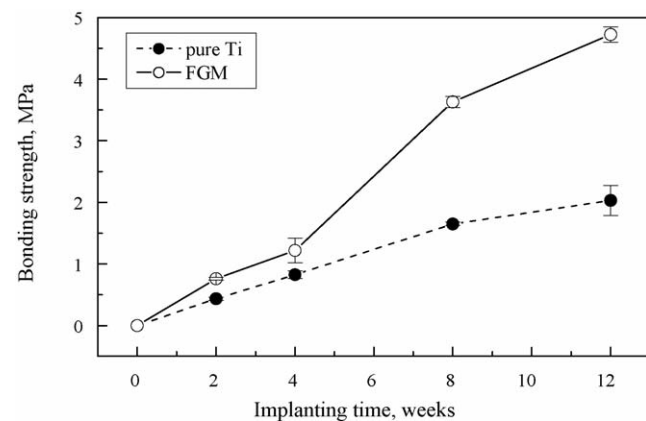


Fig. 7. Changes of shear bonding strength between bones and the implants with the implanting time.

Fig. 9 shows the shear fracture surface morphology of the implants at 3 months *in vivo*. It could be found from Fig. 9a that the shear fracture occurred mainly at the interface between pure Ti implants and new bones. The machining nicks existing on the surface of Ti metal implants before the implantation could also be found. As shown by Fig. 9b, the shear fracture for Ti-40 vol.% HA graded layer in the FGM implants occurred mainly in new bone tissues zones near the interface between the FGM implants and bones tissues. The fracture surface on the FGM implants was covered with new bone tissues, which indicates that the bonding strength of Ti-40 vol.% HA graded layer in the FGM at 3 months *in vivo* could even exceed the shear strength of new bone tissues. Ti grains on the surface of Ti-40 vol.% HA graded layer in the FGM are visible, which may be due to the poor bond between bone tissues and Ti components in the FGM.

The FGM consists mainly of Ti metal and HA ceramic. Thus the bonding mechanism of the FGM with bone tissues combines the characteristics of pure Ti metal and the ones of HA ceramic, especially for the graded layers mixed by HA and Ti in the FGM. The oxide films on the surface of Ti metal component in the FGM implants can promote the deposition of  $\text{Ca}^{2+}$  and  $\text{PO}_4^{3-}$  in body fluid or blood at the interfaces between Ti metal and bone tissues, which can result in the bond of Ti metal

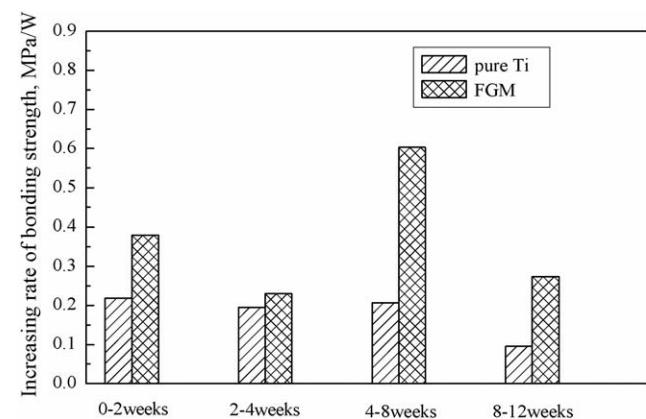


Fig. 8. Increasing rate of bonding strength of the implants in different implanting periods.

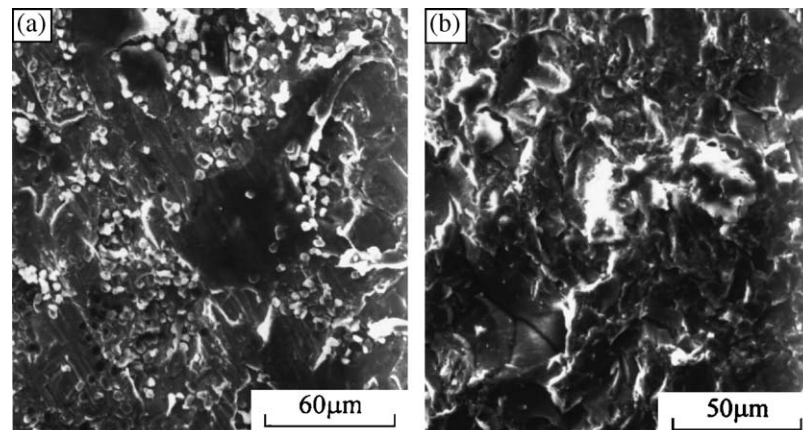


Fig. 9. SEM morphology of shear fracture surfaces of the implants after the implantation of 3 months. (a) Pure Ti and (b) Ti-40 vol.% HA graded layer in the FGM.

component with bone tissues [7]. HA component of the FGM has the similar chemical compositions and crystal structures to the mineral constituents of bone tissues [1–5]. Moreover, the biodegradable  $\alpha$ -TCP and  $\text{Ca}_4\text{O}(\text{PO}_4)_2$  phases in HA component also redound to the inlaid growth of bone tissues into the surface of the graded layers mixed by HA and Ti in the FGM implants. As a result, the bonding interfaces of Ti-40 vol.% HA graded layer in the FGM implants with new bone tissues were unclear and the FGM was osseointegrated fully with bone tissues after 8 weeks in vivo (Fig. 6d). The growth of bone tissues into the surface of the implants can strengthen the bond of the FGM with bone tissues. Thus, the interfacial bonding strength of the FGM could even exceed the shear strength of new bone tissues, which lead to the shear fracture in new bone tissues zones near the interface between Ti-40 vol.% HA graded layer in the FGM and bone tissues as shown in Fig. 9b. Obviously the FGM has better osteoconduction and osseointegration abilities than Ti metal, especially during the early stage after the implantation, which may be due to the existence of the graded layers mixed by HA and Ti in the FGM.

#### 4. Conclusions

Ti/Ti-20 vol.% HA/Ti-40 vol.% HA FGM was fabricated by a hot-pressing technique. The microstructure of sintered FGM varied gradually from Ti side to Ti-40 vol.% HA side with a graded distribution of each element. It has better biocompatibility and osseointegration abilities than Ti metal, especially during the early stage after the implantation, which can be due to the existence of the graded layers mixed by HA and Ti. There are some fibrous tissues existing at the partial interface between pure Ti implant and newborn bone at 4 weeks in vivo. By contraries, new bone tissues can contact directly with Ti-40 vol.% HA graded layer in the FGM at or after 4 weeks in vivo. After 8 weeks, the bonding interfaces between Ti-40 vol.% HA graded layer in the FGM and new bones cannot already be distinguished and the FGM was osseointegrated fully with bone tissues into one bony body. During all implanting periods, the increasing rate of bonding strength for the FGM is higher than that of pure Ti.

At 3 months in vivo, the bonding strength of the FGM implants is further higher than that of pure Ti implants and exceeds 4.73 MPa. The shear fracture for Ti-40 vol.% HA graded layer in the FGM implants occurred in new bone tissues zones near the interface between the FGM implants and bones tissues, which indicates that the bonding strength of Ti-40 vol.% HA graded layer in the FGM could even exceed the shear strength of new bone tissues after 3 months in vivo. Therefore, Ti/Ti-20 vol.% HA/Ti-40 vol.% HA FGM is a promising biomaterial for hard tissue replacement, e.g. artificial tooth roots.

#### Acknowledgements

The authors are grateful to Prof. S.Z. Xing, Department of Oral and Maxillofacial Surgery, Stomatological Hospital, Nanjing Medical University for his kind help in part of the experimental work.

#### References

- [1] H. Aoki, Science and Medical Applications of Hydroxyapatite, JAAS, Tokyo, 1991.
- [2] G. DeWith, H.J.A. Van Dijk, et al., J. Mater. Sci. 16 (1981) 1592.
- [3] L.L. Hench, J. Am. Ceram. Soc. 74 (7) (1991) 1487.
- [4] D.F. Williams, Mater. Sci. Technol. 3 (10) (1987) 797.
- [5] W. Suchanek, M. Yoshimura, J. Mater. Res. 13 (1) (1998) 94.
- [6] W. Bonfield, in: P. Ducheyne, J.E. Lemons (Eds.), Bioceramics: Materials Characteristics vs. In Vivo Behavior, vol. 523, Annals of New York Academy of Science, New York, 1988, p. 173.
- [7] R. Van Noort, J. Mater. Sci. 22 (1987) 3801.
- [8] K. Wang, Mater. Sci. Eng. A213 (1996) 134.
- [9] A. Bishop, C.Y. Lin, et al., J. Mater. Sci. Lett. 12 (1993) 1516.
- [10] C.L. Chu, J.C. Zhu, et al., Mater. Sci. Eng. A316 (2001) 205.
- [11] C.L. Chu, J.C. Zhu, et al., Mater. Sci. Eng. A348 (2003) 244.
- [12] H. Kimura, K. Toda, Powder Metall. 39 (1) (1996) 59.
- [13] S. Kirihara, et al., Mater. Trans. JIM 38 (7) (1997) 650.
- [14] A. Tampieri, G. Celotti, et al., J. Mater. Sci.: Mater. Med. 8 (1997) 29.
- [15] D.M. Liu, J. Mater. Sci.: Mater. Med. 8 (1997) 227.
- [16] I.H. Arita, V.M. Castano, et al., J. Mater. Sci.: Mater. Med. 6 (1995) 19.
- [17] B.C. Wang, E. Chang, et al., Surf. Coat. Technol. 58 (1993) 107.

- [18] A.J. Ruys, A. Brandwood, et al., *J. Mater. Sci.: Mater. Med.* 6 (1995) 297.
- [19] S.W. Ha, R. Reber, et al., *J. Am. Ceram. Soc.* 81 (1) (1998) 81.
- [20] P. Frayssinet, F. Tourenne, et al., *J. Mater. Sci.: Mater. Med.* 5 (1994) 11.
- [21] H.P. Yuan, Z.J. Yang, et al., *J. Mater. Sci.: Mater. Med.* 9 (1998) 723.
- [22] S. Raynaud, E. Champion, et al., *J. Mater. Sci.: Mater. Med.* 9 (1998) 221.